Methods of Modern Aircraft Structural Health Monitoring and Diagnostics of Technical State

Yury A. Svirskiy, Andrey A. Bautin, Ljubisa Papic and Irina V. Gadolina

Abstract This chapter provides an overview of the most relevant methods for monitoring the integrity of structures made of isotropic (metals and alloys) and anisotropic (polymer composite) materials, which are widely used in the manufacture of parts and construction structures in the modern industry. Special attention is paid to ensuring the safe operation of aircraft structures, the use of onboard monitoring systems which will allow to reduce economic costs in the near future and to increase flying safety. The paper describes different variants of implementation of the onboard recording systems of data in the analysis of the actual state of the elements of the air frame. The advantages are shown, due to which the construction monitoring will be able to replace the existing system of provision and supporting of the airworthiness, implemented through periodic inspections.

Y.A. Svirskiy · A.A. Bautin (✉)
Central Aerohydrodynamic Institute (TsAGI), Zhukovsky, Russia
e-mail: andrey.bautin@tsagi.ru

Y.A. Svirskiy
e-mail: yury.svirsky@tsagi.ru

L. Papic
Faculty of Technical Sciences Cacak, University of Kragujevac, Serbia and DQM Research Center, Prijevor, Serbia
e-mail: dqmcenter@mts.rs

I.V. Gadolina
Mechanical Engineering Research Institute of Russian Academy of Science (IMASH RAN), Moscow, Russia
e-mail: gadolina@mail.ru

© Springer International Publishing AG 2018

M. Ram and J.P. Davim (eds.), *Diagnostic Techniques in Industrial Engineering*, Management and Industrial Engineering, https://doi.org/10.1007/978-3-319-65497-3_1

1 Introduction

In the last two decades, automated structural health monitoring (SHM) systems were developed and widely implemented in the most technically developed countries of the world. The SHM means the continuous and autonomous monitoring of damage, loading, the environmental parameters, and interaction of structural elements with the environment by means of permanently attached or embedded sensor systems ensuring the integrity of the structure [1]. After a successful approbation for land-based structures (bridges, power elements of high-rise buildings, etc.), SHM methods began to be introduced in aviation. In the 90s of the last century, the Airbus company with the purpose of increasing the strength, reliability, and durability of aircraft structures and reducing the downtime of aircraft and the cost of their maintenance started to develop common approaches on creation of the SHM system for aircraft plane (A/C) within the framework of the "philosophy of intelligent aircraft structures" [2]. The Aerospace Industry Steering Committee SHM-AISC was established in 2007. It is responsible for coordinating the development and implementation of automated onboard systems for monitoring the design integrity of aircraft and reusable orbital carrier with the use of networks of embedded sensors. The International Council of Management SHM-AISC includes such companies and organizations as Airbus, Boeing, BAE Systems, Embraer, Honeywell, Aviation Administration of the USA and Europe, as well as the scientific laboratory of the US armed forces, NASA, and some leading universities [3].

Operation of the structural health monitoring systems involves the installation of different types of sensors on the structures to determine the effects of physical (humidity and ambient temperature) and power (static, cyclic, impact, and other types of loads) actions on their strength and durability [1, 4, 5].

The ultimate goal of these developments is the creation of an artificial intelligence system, which is supposed not only to be able to detect defects and malfunctions, but also to respond adequately to defects' presence and to provide appropriate recommendations to the service personnel [2, 4].

The development of the health monitoring system is divided into several stages corresponding to the system generations. These stages are close to the stages that are considered by leading aviation firms like Airbus and Boeing up to the numbering of stages and minor details [2].

- At the first stage (zero and first generation), the SHM systems are used at the structures' testing, their maintenance, and restoration. These trials also serve to test different sensors and monitoring systems in terms of their applicability to real structures. The zero-generation SHM systems are widely used in ground tests of the aircraft in our days. As an example, the SHM has been used at the certification testing on the Airbus A380 [2].
- The next stage of the SHM systems development (the second generation) is characterized by the use of sensors, information from which is read after the flight or during maintenance. While ensuring an adequate level of sensors'

reliability, it is planned to pass to sensors operating in real time, i.e., recording and transmitting information during the flight.

- The full integration of the SHM systems with onboard A/C computing and control system means the transition to the third and final generation. It is expected that the SHM system will be used to develop new approaches to the aircraft design that will ensure weight reduction of metal and composite structures by 15% [2].

The general condition for obtaining and processing the diagnostic information about the presence of damage in structures is the use of built-in and external sensors, nondestructive testing (NDT) devices, systems for storage, and processing of information, algorithms, and programs for decision-making. As noted in paper [6], diagnostic information is usually limited in volume and indirect. Existing nondestructive inspections do not detect all damages and cracks, which can later become the reason of failure states. There is a high probability of defects missing due to the equipment imperfection, negligence of the operator or inaccessible location of defects and the ungrounded frequency control. For example, if the frequency of inspections is inconsistent with the timing of initiation and propagation of fatigue cracks, it can lead to the formation of defects of critical size and consequently to the destruction of the structure [7]. Thus, the data on loading regimes provide a valuable additional source of information on the technical condition of structures. On the basis of these data using various numerical schemes, it is possible to identify the load history of the test unit and the degree of damage accumulated during its service. While comparing the results of damage evaluation with the diagnostic data of the technical condition of constructions, the parameters are estimated which have not been identified with sufficient accuracy in the previous stages. Thus, two sources of information—diagnostic data on the state of the object and data on the loading history for metal structures—are closely related and mutually dependent [7]. For the construction of the polymer composite materials (PCM), the additional information of impact damage and its intensity is more important. The solution to the problem of obtaining such information, its processing and decision-making about the maintenance strategy of an individual sample of A/C and prediction of its residual life should be implemented in the framework of integrated intelligent systems, which monitor the A/C structural integrity [8]. It should be pointed out that the important part of the SHM system creation is to develop the standards, defining rules, procedures of use, and decision-making about receiving information from them.

2 A Brief Overview of Sensors Used

The sensors development is moving in the direction of the technologies through which it is possible to detect various types of practically important damages such as cracks, corrosion, the breach of adhesion, laminations, impact damages, etc. in

metal and composite materials. The main requirements are as follows: small size and weight, ease of installation or adaptability, durability, and reliability. Currently, these requirements are satisfied by a number of sensors, which are based on different physical methods [9]:

- Acoustic emission (AE): Passive transducers listen to matrix cracking, lamination, and fiber breakage;
- Acousto-Ultrasonics (AU): A grid of piezoelectric sensors sends and receives ultrasonic pulses and analyzes changes in impulses patterns to identify and describe the damage;
- Comparative vacuum monitoring (CVM): The smallest air flow can be detected by leakage failure between atmospheric pressure and vacuum because of the crack in the matrix;
- Comparative vacuum monitoring through the thickness (CVM-TT): Using the drilled holes with a diameter of <1 mm, it is possible to reveal a breach of adhesion and lamination using the principle of similar systems in CVM;
- Crack wire sensors (CW): The break due to the occurrence of cracks or other damage serves as an alarm;
- Electromagnetic interference sensors (EMI): The system applies the built-in piezoelectric sensors and signal level analyzer. Increasing the level of signal relative to baseline values due to grease contamination or moisture indicates the presence of stratification;
- Eddy testing foil sensors (ETFS): Sensors generate a field of eddy currents in conducting materials which are violated by the cracks and corrosion damage;
- Fiber Bragg grating (FBG): The most used method of FBG is its use for measurement of temperature, strain, and vibration;
- Imaging ultrasonics (IU): Miniature, integrated network of sensors generate a signal through the material of the structural member. Changes in the reflected signal indicate the discontinuity or damage;
- Strain gages (SG): Using traditional strain gages to determine the strain.

Also, the new types of sensors are developed, in particular:

- Micro- and nanoelectromechanical systems MEMS and NEMS (microelectromechanical systems—MEMS, nanoelectromechanical systems—NEMS) (see Fig. 1);

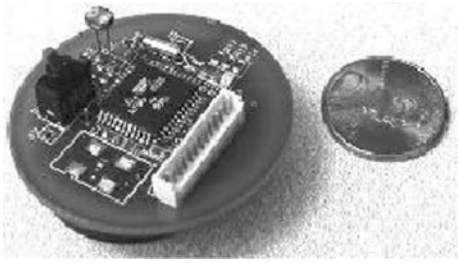

Fig. 1 Example of a MEMS sensor (≈16 cm^3), including a wireless telemetry system, microprocessor, sensors, and power supplies

- Sensors on the basis of printing conductive ink (printed conductive-ink sensors).
- Other types of fiber-optic sensors, including ones for registration acoustic emission signals [10] and for their use as sensors of cracks, use the effect of Rayleigh scattering (Rayleigh scattering). The FBG sensors are also used in conjunction with piezoelectric sensors [11]. In Ref. [11], it is noted that the measurement of deformation using FBG for the detection of damage caused by impacts is not effective enough. To illustrate, there is the following data. The impact energy of 40 J has caused significant damage but did not cause change of deformation at a distance of 40 mm from the point of impact. Reliably measured changes in the deformation caused by impact energy 30 J were localized at a distance not exceeding 20 mm.

Table 1 lists the applications of the main types of sensors (VV indicates that the sensor suits the best for this type of damage).

We should also add the conventional sensors of displacement, acceleration (accelerometers), and temperature to this list. They are used in the following methods [12]:

- Stiffness monitoring: This enables the damage stages to be identified and any deflection limit to be maintained. For coupons, changes in the modulus can be determined from the stress–strain curve, either during fatigue testing or by static loading.
- Load–deflection curve (hysteresis) monitoring: For composites, the internal damping is much higher than in metals and is an indicator of damage in the material.

Table 1 Applications of the main types of sensors

Damage type	Sensor type										
	CVM	ETFS	AE	IU	CW	IDDS	AU	FOS	EMI	CVM-TT	SG
Crack detection and evaluation	VV	V		V							
Rupture detection and evaluation	VV			V	V						
Impact detection and evaluation			VV			V		VV			
Delamination detection and evaluation			V	V			VV	VV		V	
Adhesion quality assessment								VV	V	VV	V
Monitoring of sticky repair pads								VV		V	V
Disorders of adhesion detection and evaluation			V					VV		VV	
Deformation/strain monitoring								VV			VV

- Resonant frequency and natural frequency monitoring: They provide information at a global level of the state of the material or structure at microlevel.
- Temperature monitoring: Damage induced in composites will generate heat, and as these materials have poor conductivity, it should be generally easy to detect. Infrared emissions can be detected with a suitable camera and will locate the areas of damage and how these will grow. Thermocouples are simple to install and have been placed in locations where high strains have been detected, possibly by a strain analysis.

In many cases, the sensors are combined in a distributed network, the use of which is performed in three ways [9]:

1 By the place of installation: The sensors are just the objects which are set on the construction in this case. The reading is collected manually using an external measuring system through the selected interval.
2 A network of sensors at the place of installation: In this case, the sensors are complemented by miniature measurement electronics. Stored data are periodically collected by the technical staff on the ground.
3 Wireless network sensors: Electronics provides wireless transmission of data as a development of the second method. Systems receiving this data diagnose construction in real time. The telemetry system gives the possibility of continuous wireless data transmission in the air or on the ground to a remote site. The Web site can be programmed to data scan, the determination of the threshold of structural damage, and informing staff about the need for repairs or other maintenance.

Currently, SHM systems have become a standard tool in the certification of static and fatigue full-scale tests of air constructions [9]. It reduces the switching-off of testing for control of the selected zones. For example, sensors of acoustic emission (Physical Acoustics Corp. (PAC, Princeton Junction, NJ, USA)) were used to monitor carbon horizontal stabilizer during field tests of the wide-bodied Boeing 777. Also, the AE systems were used for static tests on critical load and destruction for the identification and assessment of subcritical damage propagation and determination of a sequence of destruction of individual elements of the design.

Similarly, during the full-scale fatigue testing of the Airbus A380 in Toulouse (Toulouse, France) conducted by IABG (Dresden, Germany), 47500 flights were made during 26 months using a variety of health monitoring system (HMS) sensors, including the vacuum systems CVM, eddy current foil sensors (ETFS), AE sensors, and crack wire. Installed on the fuselage and wings, these HMS provided detailed information on crack generation in aluminum airframe, in the carbon fiber center section of the wing and parts of the fuselage made of the glass-reinforced aluminum (GLARE).

3 Methods of Location of Impact Damage Based on the Analysis of the Response of Polymer Composite Materials' Structures

The problem of damage detection and determination of their parameters in aircraft construction is a difficult task even for ground services. In this regard, for SHM systems the urgent task is not only to detect the damage but also to detect the fact of impact damage. It can be done monitoring the structural elements response to the impact. The fact of an impact serves as a signal to an extraordinary nondestructive testing of the integrity of the structure.

The problem of impact damage detecting on the response to the impact of structural elements of onboard monitoring system includes the following subproblems:

- Identification of the point of impact;
- Evaluation of damage parameters from impact;
- Determination of impact parameters.

Conventionally, the approaches to solving these subtasks can be divided into two types:

1 Creating the most accurate mathematical model which predicts the properties of the structure ("theoretical" approach) and
2 Conducting a large number of experiments and then predicting the properties of the structure via interpolation of data obtained in such experiments ("calculation-experimental" approach).

Due to the fact that the construction of sufficiently accurate models of complex aircraft constructions suitable for the SHM systems is currently unrealizable, the most popular is the "theory-experimental" approach.

Let e(i, t) be the deformation of the i-th sensor at time t, e_t is the vector composed of such deformations. Suppose that at time t = 0 the impact occurred, and at times t = 0, …, t = ∞ of the sensor readings were taken. In the general case, the dependence of the impact force at the moment t at point x would be as follows:

$$F_{xt} = f_t(e(t = 0), e(t = 1), \ldots, e(t = \infty)) \tag{3.1}$$

In the simplest cases (infinite perfectly rigid one-dimensional rod, two-dimensional infinite surface, the infinite speed of sound, etc.), the dependence f_t takes the simple enough forms. In such cases, we may build the appropriate mathematical model to determine the coordinates of the impact. So, in an environment with an infinite speed of sound and a very fast damping of the oscillations, members with t > 0 can be neglected, and dependence (3.1) takes the form:

$$F_{x0} = f_0(e(t = 0)) \tag{3.2}$$

However, in the case of the arbitrary configuration construction assembled from materials with random properties, the dependence of (3.1) is very difficult. In this case, the main factors preventing the creation of effective mathematical models are as follows:

- The complexity of mathematical modeling of composite materials and complex parts from them;
- The complexity of modeling processes in various joints of complex structures;
- Difficulties in modeling the construction made from various materials.

In this regard, in practice, there are various ways of overcoming the above difficulties.

3.1 Simplified Model Methods

In work [13], it was proposed to localize the point of impact according to a highly simplified mathematical model: The distance from sensor p_i to the impact point x is proportional to the maximum amplitude: $|x - p_i| \sim \max(e_{i,t=0}, \ldots, e_{i,t=\infty})$. In work [13], this model was checked experimentally, but the results were not satisfactory. In this regard, there is a reason to believe that the approach of using a deliberately simplified model is unsatisfactory.

Another common method of finding the point of impact is the method of time delays: It is supposed that the disturbance comes faster to the sensors located closer to the point of impact. This method is also unsatisfactory for complex anisotropic structures.

There are other approaches to finding the point of impact, based on simplified mathematical models: the measurement of power distribution [14], etc.

3.2 Linear Stationary System

One of the most promising approaches is the approach given in [14, 15]: a representation of the model in the form of a linear stationary system. In this case, a minimum number of initial assumptions are used: linearity (deformation of the i-th sensor is proportional to the impact force) and time invariance (a delay of indications of the i-th sensor relative to the exposure time is fixed). In such a system, the deformation depends on the strength in the following form:

$$e(i,t) = \sum_{k=0}^{t} h(i, k)F(x, k - t) \tag{3.3}$$

where F(x, t) is the force at point x at time t, h(i, t) is the transition function.

In matrix form, this equation can be written in the form:

$$e(i) = H(i)F_t(x) \tag{3.4}$$

where H is the lower triangular matrix composed of the transition functions of this linear system, F_t is a vector of power values at points in time t.

Thus, the problem is reduced to the following stages:

1 Definition of the matrix H: While doing this, it is necessary to use the experimentally obtained compliance of the strains e(i, t) on the history of the loading F (x, t). Using these data and using the least squares method, we can find the desired transition functions.

$$\sum (e(i) - H(i)F_t(x))^2 \rightarrow \min \tag{3.5}$$

2 The definition of the point of impact x was found by means of transition functions: Assuming the setting of force $F_0(t)$ is known, we solve the minimization problem (3.5) for all x;

3 Determination of the settings of the force F(t): Using the properties of linearity of our system, we find the inverse transition matrix H′, such that

$$F_t(x) = Y'(t) \cdot e(t) \tag{3.6}$$

Assuming that the impact location is known, we find the history of loading by the formula (3.6);

4 Alternately, assuming that the point of impact and the load history are known, we solve tasks p. 2 and p. 3 by mean of iterations. Eventually, the solution is converged.

3.3 The Dynamic System

The most promising approach for the recovery of impact force by sensor readings is a representation of the model as a dynamic system [13], because during the impact the condition of linearity and stationarity of the system typically fails. According to the theorem of Takens [16], it is possible to recover the properties of the random smooth dynamical system without knowing its exact mathematical model. It is done according to the following algorithm:

1 Selection of parameters τ (time, seconds) and D (constant): Parameters can be chosen arbitrarily, but in that case good results are not always obtained. In practice, some empirical assumptions are often used;
2 Let E(i, t) be matrix function of time t composed of sensor readings in some points of time.

$$E(i, t) = (e(i, t), e(i, t + \tau), \ldots, e(i, t + \tau(D - 1))) \tag{3.7}$$

3 In our dynamic system, the matrix will depend on the force of the impact at the point x at time t: E(i, t) = f(F(x, t)).

Next, we need to obtain the dependence of f.

$$\sum (E(i, t) - f(F(x, t)))^2 \rightarrow \min, \text{ (for all i, x, t)} \tag{3.8}$$

Usually, neural networks are used for the approximation of such high-dimensional functions. In work [14] for the approximation of f, the support vector machines were used.

3.4 Method Using Neural Network

The results of the method of determining the coordinates and power of the impact using a neural network developed by Rybakov are presented in work [17]. The method was applied to the specimen, which was a square 200 × 200 × 3 mm of the combined composite material. Layers of carbon and fiberglass are alternated in the specimen. Three (directed along axes *X*, *Y*, *Z*) piezoelectric IPC accelerometers were attached at the specimen at each points 1, 2, 3, 4 (see Fig. 2), a total of 12 sensors, for registering acceleration.

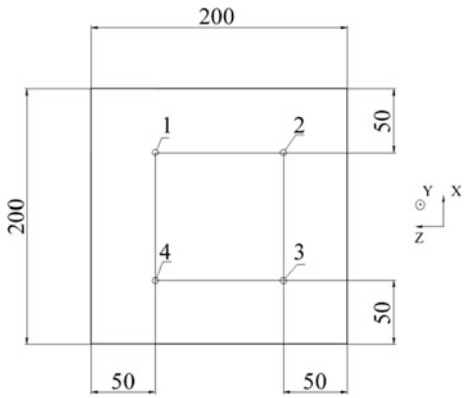

Fig. 2 Location and the directional axis of the sensor

The specimen was fixed on the edges. A hammer was used to strike and check force. The hammer was secured in a homemade impact machine for the replicability of frequency of occurrence of energies and angles of impacts. Impacts were made at random points with uniform distribution on the sample surface with different energies A, B, C at an angle of 90° to the surface. Also, the impacts were carried out with different heads on the hammer. The steel head made 10 impacts; a plastic head was made 230 impacts; and a rubber one made 160 impacts. Data logging was carried out using the LMS data acquisition system at a frequency of 51200 Hz.

3.4.1 A Dynamic System Construction

The approximation of properties of the specimen was conducted by means of restoration of properties of the corresponding dynamic system. For this purpose, the corresponding vectors of the phase space were built (1.7) $E(i, t) = (e(i, t), e(i, t+\tau), \ldots, e(i, t+\tau(D-1)))$ at the moment of contact upon impact (3–10 ms).

The parameters τ, D are selected according to the maximum and minimum frequencies of the spectrum of sensor values at the moment of impact. A typical spectrum at the moment of contact upon impact of the tested plate is as follows (Fig. 3):

It is shown that significant signal frequencies are in the range from 600 to 6000 Hz. The time discretization was chosen with the focus on the theorem of Nyquist–Shannon [18]: To restore the dependency, it is necessary to take it equal to half of the minimum period of significant frequencies of the signal. Accordingly, $\tau = 0.5/6000\ \text{s} = 8.3\times10^{-5}\ \text{s}$.

Dimension of constant D was determined on the basis of the empirical assumption that the vector of the phase space should cover at least the minimum period of all significant frequencies of the signal.

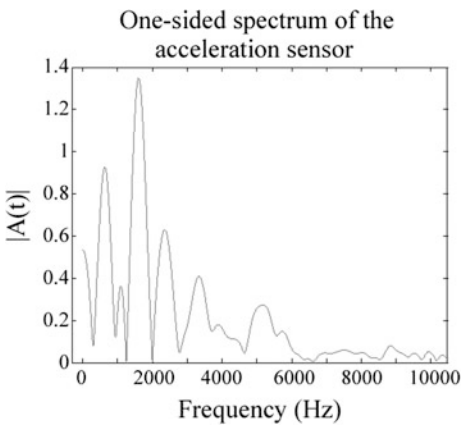

Fig. 3 Spectrum at the moment of contact upon impact, 3 ms

3.5 System Properties Restoration by Means of Neural Networks

The properties of the dynamic system were approximated by a back-propagation neural network [19]. The input of the network was supplied by vectors $E(i, t) = (e(i, t), e(i, t+\tau), \ldots, e(i, t+\tau(D-1)))$. A total of $D \times N$ input neurons were used (D = 10 is the dimension of embedding, N = 12 is the dimension of the data vector at the particular moment of time, i.e., the number of sensors).

The output was supplied by the registered values of power F, the X, Y coordinates: a total of three output neurons.

Several different existing variants of back-propagation algorithm were tested. The best results (by far) were obtained during the training using the optimization of Levenberg–Marquardt [20]. The training was applied to 70% of the data of the entire set of data for inputs and outputs of the network, and testing was carried out on 30% of the data.

As a result of training, a neural network was obtained which is able to restore the history of loading at the moment of impact and the point of impact.

An example of a graph of restored power is shown at Fig. 4. The exact values of power cannot be restored; however, the general trend can be seen clearly.

Figure 5 shows the experimental and calculated coordinates of the impacts. The distance between the real and the estimated points is 14 ± 12 mm.

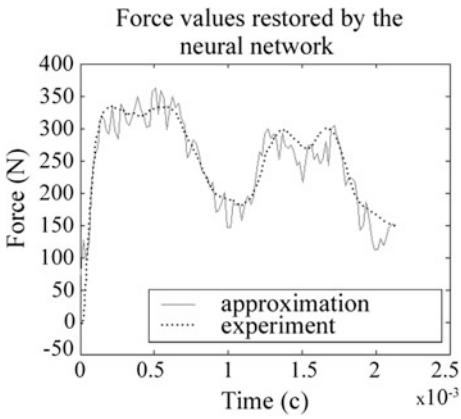

Fig. 4 Graph of power at the moment of impact restored by neural network

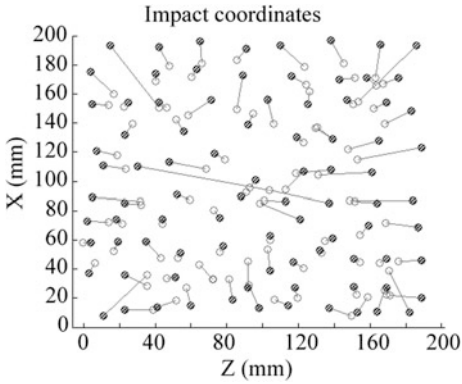

Fig. 5 Coordinates of the impacts (striped markers are experiment, white ones are calculation)

3.5.1 Restoration of Properties by the Support Vector Machine System

The support vector machine [21] is a promising algorithm for optimization and classification of the data that is rapidly developed recently. In this work, it was attempted to use the support vector machine for the purpose of approximation of properties of the achieved dynamic system. We used the library LibSVM in this work. The input of each machine was supplied by vectors $E(i, t) = (e(i, t), e(i, t + \tau), \ldots, e(i, t + \tau(D - 1)))$. The output of the first machine was supplied with power, the output of the second machine was supplied with X-coordinate values, and the output of the third machine was supplied with Y-coordinate values.

For the purpose of training, the supported vector machines with kernels were used:

- Radial basis function (RBF);
- Heterogeneous polynomial kernel.

When using the machine with kernel-RBF, the convergence was very fast, but error at the end of training was much higher than in the case of a neural network (under fitting).

In case of polynomial kernel, the convergence rate was also very high. However, such machines have been overfitting (the error rate was too low on the learning set, and the high one was on the test set). Attempts to apply the cross-validation resulted in underfitting again.

Thus, it is necessary to conduct further researches of support vector machine, which has two advantages:

- High speed of convergence;
- The existence of local minima does not impede the determination of the optimal solution, which provides a higher reliability of the results.

Fig. 6 Benefits of HMS

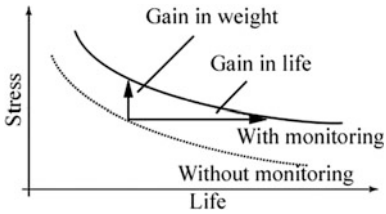

4 Development of Methods of Damage Detection Based on Results of Measurements of Local Stress–Strain State Kinetics

4.1 Problem Formulation and Analysis of Existing Methods of Monitoring of Polymer Composite Materials Structures

Currently, the miniaturization and cost reduction of the measuring and computing technology has provided the possibility of application of embedded strain gage system that allows to determine the local stress–strain state accurately. Conventional strain gages as well as of becoming more widespread fiber-optic sensors of strain and temperature can be used. With their help, as the results of a number of studies show, it is possible not only to determine the service loading data of the structure, but also to discover the damages in the main load-bearing elements

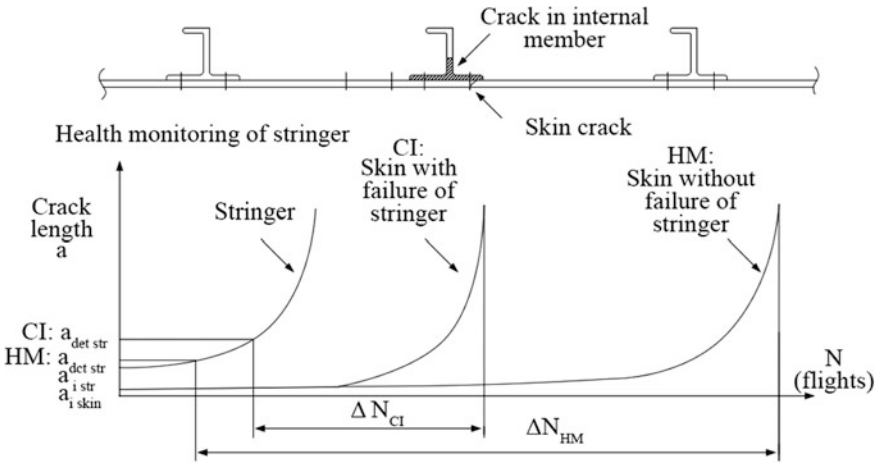

Fig. 7 Comparison of periods of crack propagation in case of absence and presence of SHM system (*NDM*—nondestructive monitoring)

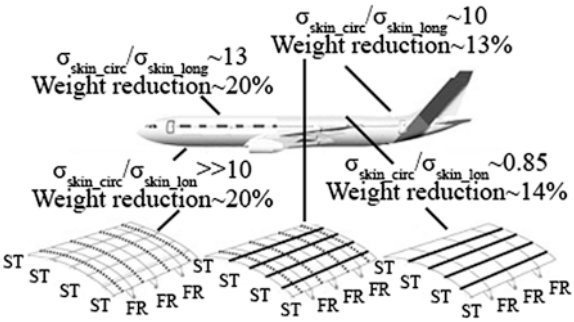

Fig. 8 Analysis of the possibilities of weight reduction for the various fuselage elements and the location of SHM sensors necessary for that [18]

of constructions. In this section, we examine works carried out in this direction and methods which can be used for their practical implementation.

The work [22] shows that information about the integrity of the main reinforcing element, for example, stringer, allows to increase the interval between inspections or reduce the weight (Fig. 6).

The increase of the interval between inspections is achieved due to the fact that the duration of crack propagation in case of non-failured stringer is substantially increased (Fig. 7) [23].

The advantage in weight is achieved due to the fact that if there is the SHM it is possible just to provide structural strength at much less lengths of the cracks.

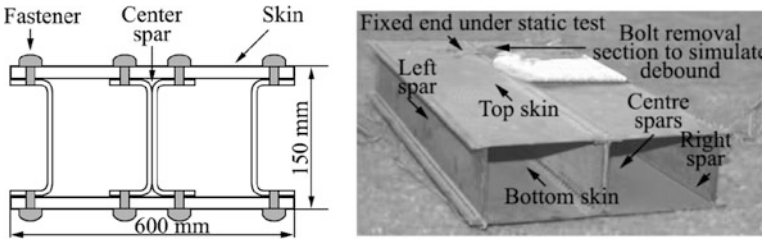

Fig. 9 Scheme (left) and photograph (right) of the examined fiberglass PCM construction with bolting connection

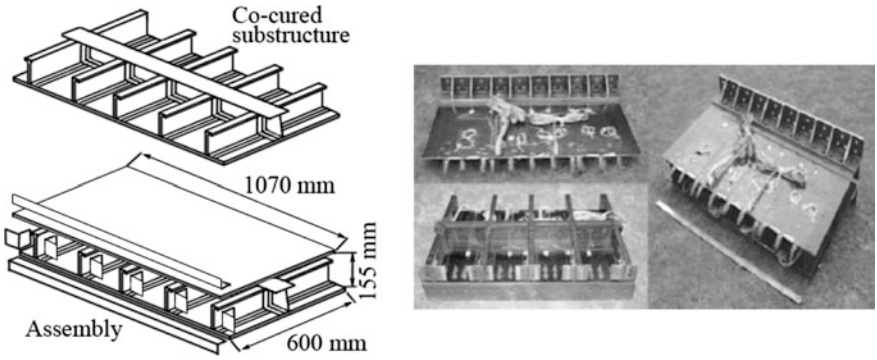

Fig. 10 Scheme (left) and photograph (right) of the examined carbon fiber PCM construction

Figure 8 shows the results of the analysis carried out for the wide-body passenger aircraft of a medium action radius which is made of aluminum alloy 2024. Sensors of monitoring of stringers' integrity are indicated by the solid lines, and sensors of monitoring of shell integrity are indicated by the dashed lines. Symbols: ST—stringer, FR—frame, $\sigma_{skin_circ}/\sigma_{skin_long}$—the ratio of circular stresses of the shell to longitudinal ones.

Along with monitoring of stringers' integrity and other load-bearing elements, it is relevant for PCM structures to monitor such specific for PCM types of destruction as the lamination. From this point of view, the subject of great interest is the result of work [24], which examines the ability to detect damage by monitoring local stress–strain state (Figs. 9 and 10) in the PCM construction.

Three types of specimens were examined: fiberglass PCM testboxes with bolted joint (Fig. 9) and adhesive connection, and also carbon fiber PCM testbox (Fig. 10). The loading type was the cantilever bend.

There were three options examined upon the fiberglass PCM testboxes with bolted joint:

- Integral structure: The testbox was tested with fully installed bolts to provide a basis for comparison with damaged constructions.
- Four bolts were removed. Four pairs of bolts were removed along the central spar near the fixed edge (Fig. 11). Since the distance between the bolts was equal to 20 mm, the length of lamination was 100 mm.
- Eight bolts were removed. Eight pairs of bolts were removed along the central spar near the fixed edge. The length of lamination was 180 mm.

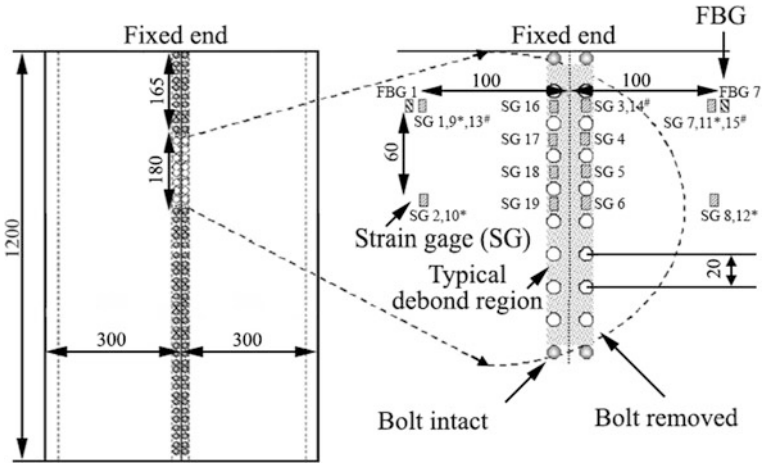

Fig. 11 Scheme of the lamination simulation of the fiberglass PCM structure with bolted joint (left). The location of the bolts and the scheme of sensors adhering (right)

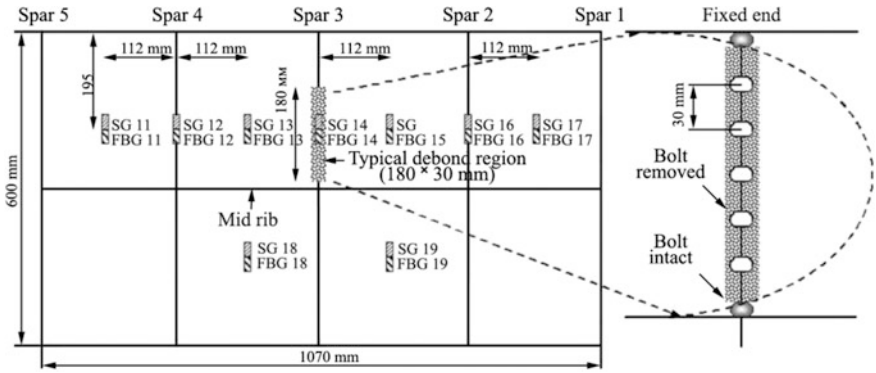

Fig. 12 Plan view of FBG and strain gage sensor location on testbox (left), bolt location on the spar for debond (right)

The width of lamination was equal to 30 mm—the width of the flange of the spar. In all three cases, deformation and displacement were measured. Figure 11 shows the schemes of the lamination simulation, the location of the bolts, and sensors' layout. The deformation was measured by both fiber Bragg grating (FBG) sensor and strain gages (SG).

One fiberglass PCM testbox with adhesive connection was made integral, and there was the simulation of 180 mm length lamination on the second one by means of the lack of adhesive connection in the same place where eight bolts were removed in case of the fiberglass PCM testboxes with bolted joint.

The carbon fiber PCM testbox was designed to test stiffness which is more typical for modern aviation structures and with the higher resistance to local buckling, particularly, due to the central rib. Lamination was simulated by

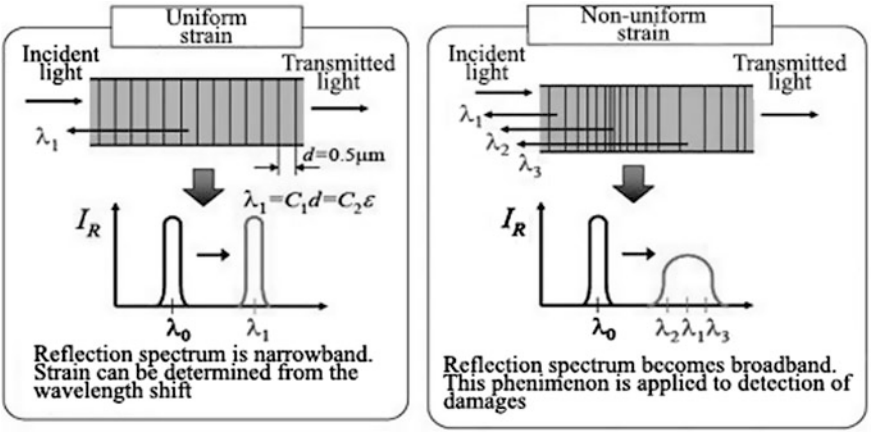

Fig. 13 Response of fiber-optic sensors with Bragg gratings under homogeneous and heterogeneous deformations

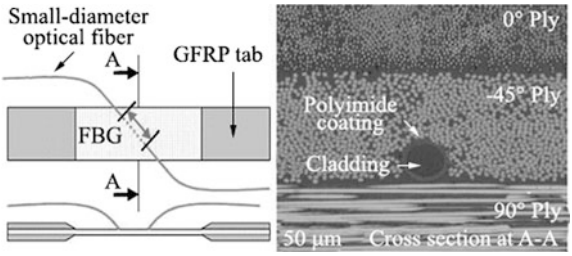

Fig. 14 Small diameter fiber-optic sensor, integrated into the layer −45° for the detection of transverse cracks in the adjacent layer 90° quasiisotropic laminate [45/0/-45/90]

removing five bolts consecutively (with a step of 30 mm), simulating 180 mm length lamination for different variants in three central spars (Fig. 12).

The main results that were obtained are as follows:

- In case of fiberglass PCM testboxes with bolted joint and adhesive connection, sensors located in the lamination zone allow to detect damage quite reliably, particularly, due to local buckling.
- In case of carbon fiber PCM testbox, sensors located in the lamination zone allow to detect damage quite reliably only if the detection is carried out by means of comparing sensor data in the same place of damaged and undamaged structure, i.e., not by absolute but by relative values of deformations.
- In addition to the deformation value, another damage indicator can be a violation of linearity between power applied and the deformation measured by strain gages as a result of local buckling (Fig. 13).

In addition, it was received:

- Removing the bolts on the fiberglass PCM testboxes allows to simulate delamination well enough; however, under the adhesive connection, local buckling occurs later and more abruptly.
- Measurement of deformation by fiber-optic sensors and strain gages gives alike results.

The subject of great interest is the work [25], which shows the possibility of detection of such defects of carbon fiber PCM as the lamination and transverse cracks due to the property of fiber-optic sensors with Bragg gratings to change the spectrum form of the output signal due to the appearance of heterogeneity caused by lamination and/or transverse cracks. However, it should be noted that the issues of practical use of this method require further study in order to provide monitoring not only of the area where the sensor is located, but also of the structure (Fig. 14).

4.2 Monitoring of Multiple Site Damages of Structures Made of Aluminum Alloys

Multiple site damages are the most dangerous type of damages in aircraft structure. Nowadays, designers of aircrafts are trying to prevent emergence of such damages

at the stage of design [26]. Major aviation accidents connected with the emergence of multiple site damages forced air operators to set a lifetime of construction elements where the multiple site damages can occur, based on the principle of "safe life," which made the operation of such aircrafts much more expensive [27].

As a solution to this problem, there is an approach nowadays connected with such structure design when it is possible to confirm experimentally the impossibility of multiple site damages in it.

This approach contradicts to the concept which has been developed over many years of designing of aviation structures without significant differences between the durability in various locations, since such a design implies the absence of unreasonable reserves of the individual elements of airframe with high service life [28].

The use of monitoring of damages, which is able to provide multiple site damages detection in time, allows to set a lifetime of construction elements, where multiple site damages can occur based on the principle of "fail safe," which will make the maintenance of modern aircraft structure more cost saving without reduction in safety level during the operation.

The use of monitoring damage, which is able to provide timely detection of multiple site damages, provides the ability to assign resource for design elements with the multiple site damage, on the principle of "fail safe" that will make the maintenance of modern aircraft design more economical, not reducing the operation safety.

4.2.1 The Results of the Monitoring of Damages During Fatigue Testing of Longitudinal Joints

While determining the fatigue characteristics of elements of prospective passenger A/C, the authors of this work had carried out the testing of the damages monitoring by means of analysis of data of strain gages.

The prototypes of samples of the longitudinal joints of the fuselage, designed to obtain fatigue characteristics and determine the optimal structure of the connection, were used for the purposes of the experiment. All the samples were represented by two sheets of the same thickness, connected to stringer by three rows of rivets (Fig. 15).

During the testing, the strain was measured having different number of operating cycles, and the damages effect on the stress–strain state of the sheets was determined. The wire strain gages were used in the experiment, which were installed in two rows at the outer rivets on two sides of the inner and outer sheets. In this case, a large number of sensors used in the experiment were due to the examination of the size of the area where the changes of stress–strain state occurred as a result of emerging damages. In close proximity with the rows of rivets, due to the limitations connected with the available space for installation, small-base sensors with a base of 1 mm were used. In the regular part of the sheets, sensors with base size of 10 mm were used (Fig. 16, sensors with a base of 1 mm are shown in gray, and the ones with a base of 10 mm are shown in black).

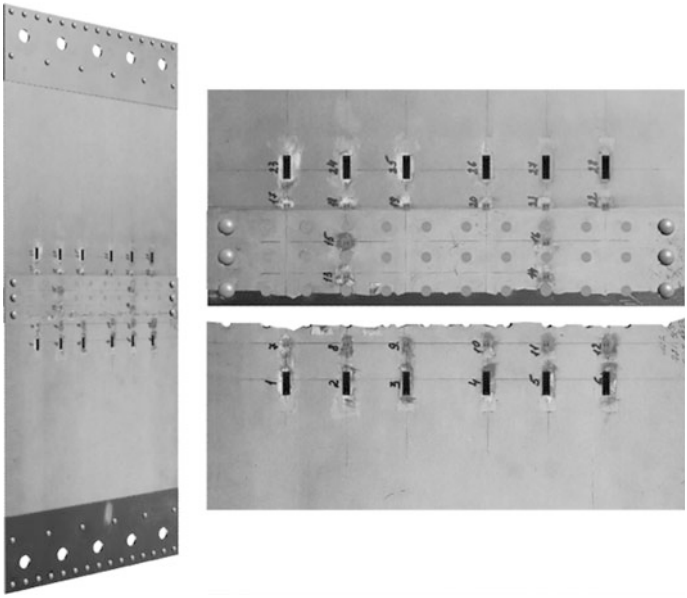

Fig. 15 Sample of the longitudinal joint of the fuselage with installed strain gages, and the specific destruction at an outer row of rivets

After the fatigue testing of the samples of longitudinal joints, the fracture surfaces of separated parts were carefully analyzed; as a result, the initial centers of cracks origin were identified, as well as the speed of cracks growth in different zones of the fracture and appearance of the fronts of cracks in different service time (Fig. 17). The received information was used to determine the zones of change of the stress–strain state by means of finite-element (FE) simulation.

The research of the longitudinal joint samples showed the following results:

- The destruction of samples in the longitudinal joint in most cases occurs in cross section that goes through the middle of the outer row of rivets on the outer connection sheet. Macropicture of fractures of the joint indicates that the emerging fatigue fractures related to the initially formed fatigue cracks are concentrated in the area of several holes. Some centers of small fatigue cracks observed in particular places of the damaged critical sections of the sample are secondary. Their initiation is triggered by increase of existing stresses due to the reduced area of the sample effective cross section during the propagation of the initially formed fatigue cracks. The initiation of all the fatigue cracks occurred on the surface of the outer sheet of the shell that contacts through the sealant layer with the inner sheet made of the same material. During almost all the period of propagation of the initial fatigue cracks, they evolved as blind cracks and could not be visually detected until the cracks became through and reached the length of reliably detectable size on the surface of the shell inverted outward

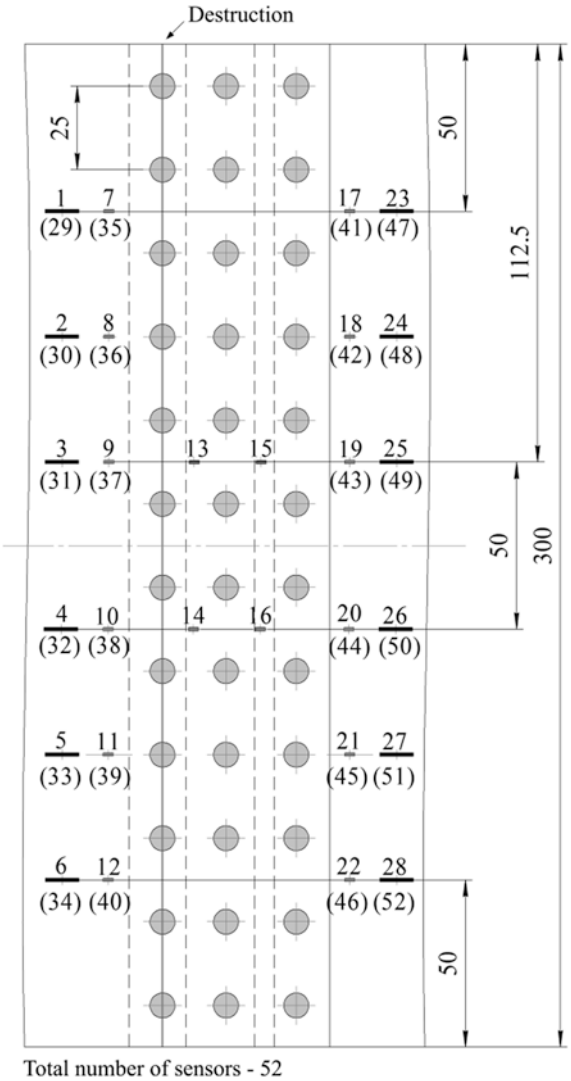

Fig. 16 Scheme of sensors' layout

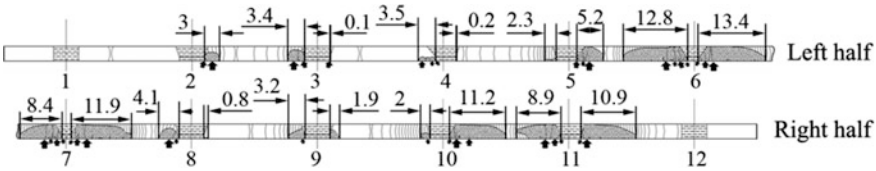

Fig. 17 Scheme of the fracture of the sample and size of the cracks (table of symbols is in the Table 2), received by means of fractography

Table 2 Table of symbols used in the diagrams of the fracture

	Arrow indicates the location of the fatigue fracture focus and the direction of propagation of closed fatigue cracks
	Fatigue zone where the crack rate is less than 5 mkm/cycle
	Fatigue zone where the crack rate is more than 5 mkm/cycle
	Rupture zone
	Hole

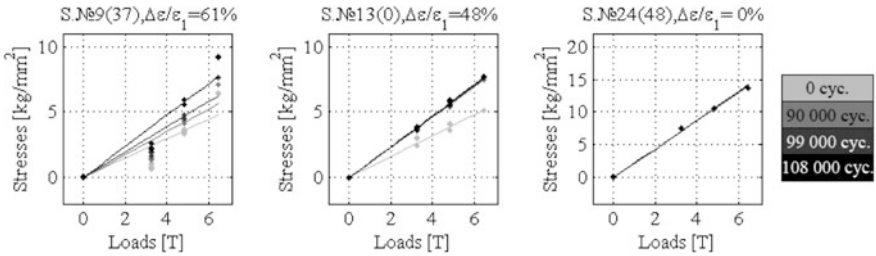

Fig. 18 Deformation change in different areas of the structure

of the fuselage. The overall unsatisfactory assessment, which characterizes possible maintenance of used longitudinal fuselage joints for damage tolerance, is caused by the poor inspection ability of the connection sheets by means of a visual control.

- Changes in the strain gage readings registered during the experiment can be divided into three groups. The first group includes the sensors located near the place of future destruction. The registered change in the strain gages readings in this group ranges from 10% to 50% and is found in all places across the width of the outer sheet used for installation of the sensors (Fig. 18, left graph). The change in the sensors' readings of this group is a result of the emergence of fatigue cracks in the structure. The second group includes sensors installed between the rows of stay bolts. There was a change in readings of this group of sensors as well, which is most likely caused by the changes in allocation of the stresses in the distances between the rows of rivets during the operating time of structure (Fig. 18, middle graph) A significant change in readings occurred in the interval between the first and second strain measurements, and further indications of the strain gages were on the same level. The third group of sensors is the strain gages which are maximally distant from the damage location. There was no change in the sensors readings of this group (Fig. 18, right graph).

The conducted experiment shows that in cases when the examination of the state of the structure by means of visual monitoring is impossible, damages in the structure can be detected by means of sensors measuring parameters of local stress–strain state.

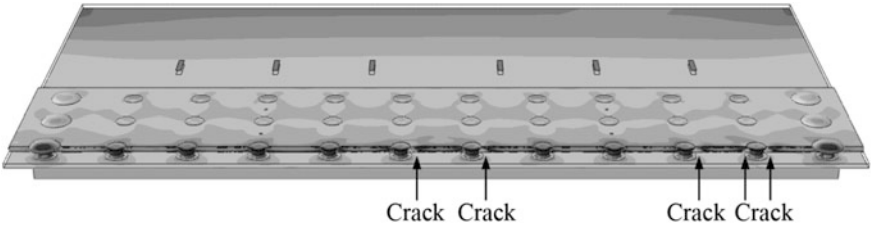

Fig. 19 Appearance of the destroyed section with a simulated crack

4.3 Analysis of the Kinetics of Stress–Strain State in the Area of Damage by Means of a Finite-element Model of the Structure

For analysis of the kinetics of the elastic deformations field, finite-element modeling was conducted by means of several FE models of three-row double-shear connection in the software package ABAQUS. The models consider the data about location of the fronts of fatigue cracks obtained during fractography of the samples during the fatigue life, when strain measurement was carried out. The model of the upper shell sheet was divided into three parts for the purpose of a correct subdivision of the simulated objects into the elements. In the geometry of the middle part,

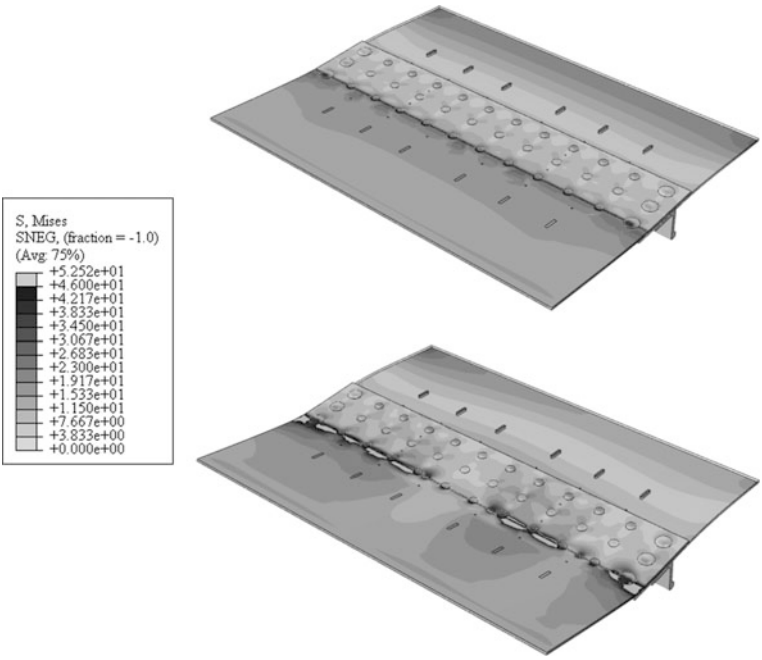

Fig. 20 FE model of the joint, calculated as for undamaged (top) and for fatigue damaged (bottom)

Table 3 Stress–strain state kinetics of the outer sheet connection

Lower surface of inner sheet	Upper surface of outer sheet
Joint fraction scheme by N = 90,000 cycles	
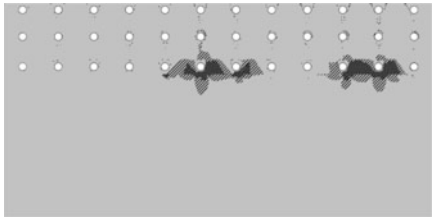	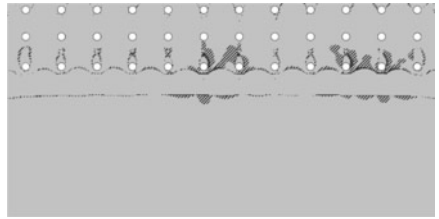
Joint fraction scheme by N = 99,000 cycles	
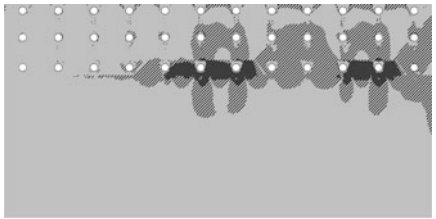	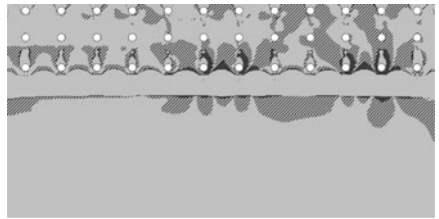
Joint fraction scheme by N = 108,000 cycles	
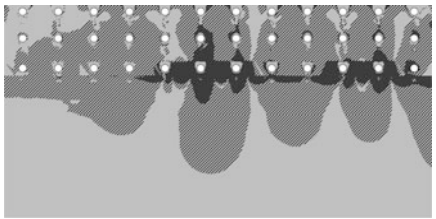	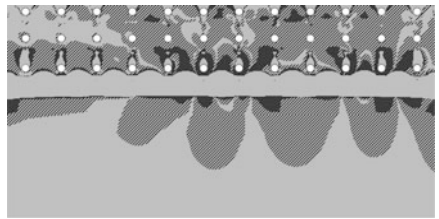

(continued)

Table 3 (continued)

Lower surface of inner sheet	Upper surface of outer sheet
Joint fraction scheme by N = 113,500 cycles	
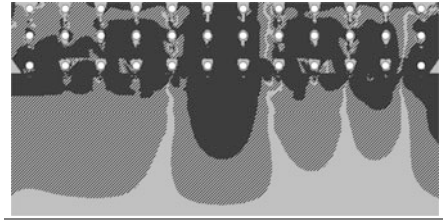	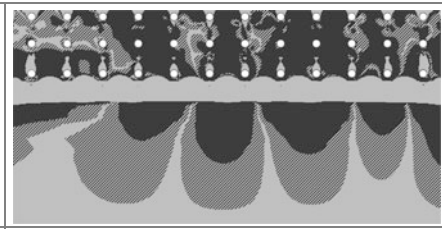
Difference, Δε [%]	~ 0 > 5 > 30

the contours of the fronts of fatigue cracks were used which were received by means of analysis of the fractures of the tested samples (Fig. 19).

Figure 20 shows the change in the stress–strain state of the longitudinal fuselage joint which was reproduced in FE models corresponding to the initial (undamaged) and the final (before destruction) state of the joint.

The kinetics of the stress–strain state of the joint is shown in Table 3, which illustrates the change of the elastic stresses field in comparison with the initial state: Light gray is no change, shaded is a change of not less than 5%, dark grey is a change of not less than 30%. In the analysis of the kinetics, it was used the data about deformations obtained on the undamaged and damaged models taking into account the size of damages corresponding to the appropriate operating time.

According to the analysis of the kinetics of stress–strain state, you can make the following conclusions:

- Extensive zones, where changes of stress–strain state have occurred, are fixed similarly well on the upper and the lower surface of the destroyed sheet;
- The damage effect can be fixed in advance. There are several variants of sensors' layout in the area of stress–strain state changes;
- When the complete destruction of the joint would be not less than 15 thousand flight cycles, the region of maximum change of stress–strain state covers about two-thirds of the width of the top sheet and is located in the third row of the outer sheet;
- For the type of fatigue fracture with multiple sites of crack initiation investigated in the experiment, it can be defined and compiled the optimum sensors' layout scheme based on the analysis of strain gages and fractography of fractures by means of FE simulations, which do not require control of the stress–strain state of a large number of places. It will guarantee the early detection of fatigue damage.
- An estimated number of required sensors, which is necessary for the detection of damages of this type, is one monitoring location for every 100 mm of width of the sheet.

The examination of the kinetics of the stress–strain state showed that the monitoring of local stress–strain state can be used in the creation of a full-sized monitoring system. This measure is intended to expand the perspectives of the whole complex of methods providing the safety and maintenance of airworthiness of civil aircraft (Table 3).

5 Conclusion

This chapter gives a short review of the various methods of monitoring the condition of aircraft structure elements, of various sensors used in modern health monitoring systems and areas of sensor's application.

It is shown that localization of impact damage on composite structures by means of the analysis of the strain gages' readings is possible. The best result in detecting the location and force of impact is obtained through the use of neural networks.

The paper presents the results of the research and application of monitoring techniques based on monitoring local stress–strain state for the detection of fatigue damage of the elements of modern aircraft structures. The effective use of strain sensors was confirmed experimentally for monitoring damage of the structures from polymer composite materials and aluminum alloys with multiple sites of crack initiations. The paper shows that the inability of visual detection of fatigue damage of a longitudinal joint of the fuselage timely can be compensated by the analysis of local stress–strain state using a small number of strain gages installed on the structure.

To determine the parameters of sensors' layout scheme for monitoring the longitudinal joint, this work represents the analysis of the kinetics of stress–strain state calculated by FE model of the structure based on the detected fatigue damages. The analysis shows that the estimated number of sensors should be based on the assumption about the location of at least one sensor for every 100 mm along the longitudinal fuselage joint or alternatively one sensor should be placed for every five holes near the outer joint row.

References

1. Chang F-K (2005) Structural health monitoring 2005: Advancements and challenges for implementation. DEStech Publication Inc, Lancaster
2. Speckmann H, Roesner H (2006) Structural health monitoring: a contribution to the intelligent aircraft structure. In: Proceedings of 9th European NDT conference, Berlin, Germany, 25–29 Sept 2006
3. Coppinger R (2007) Airbus and Boeing back structural monitoring. http://www.flightglobal.com/articles/2007/02/20/212184/airbus-and-boeingback-structural-monitoring.html
4. Bartelds G (1997) Aircraft structural health monitoring, prospects for smart solutions from a European viewpoint. NLR TP 97489 A National Aerospace Laboratory NLR 13
5. Boller C, Buderath M (2007) Fatigue in aerostructures-where structural health monitoring can contribute to a complex subject. Philos Trans R Soc Lond A 365:561–587
6. Bolotin VV (1990) Longevity of machines and structures. Mashinostroenie, Moscow (in Russian)
7. Whittingham RB (2004) The blame machine: why human error causes accidents. Elsevier Butterworth-Heinema, Burlington
8. Ignatovich S et al (2011) The perspectives of using on-board systems for monitoring of residual life of airplane structures. Vestnik TNYU (mechanics and material science). Kiev Special issue 2, 136–143 (in Russian)
9. Gardiner G (2015) Structural health monitoring NDT-integrated aerostructures enter service. Composites World, 46–49
10. Fengming Yu et al (2014) Identification of damage types in carbon fiber reinforced plastic laminates by a novel optical fiber acoustic emission sensor. In: Proceedings of the European workshop on structural health monitoring (EWSHM)

11. Gëuemes A et al (2014) Damage detection in composite structures from fibre optic distributed strain measurements. In: Proceedings of the European workshop on structural health monitoring (EWSHM)
12. Mayer RM (1996) Design of composite structures against fatigue. Applications to wind turbine blades, ISBN 0 85298 957, 11–14
13. Coelhol CK, Hiche C, Chattopadhyay A (2010) Impact localization and force estimation on a composite wing using fiber bragg gratings sensors. In: 51th AIAA/ASME/ASCE/AHS/ASC structures. structural dynamics and materials conference, Orlando, 2010
14. Park J, Ha S, Chang F-K (2009) Monitoring impact events using a system-identification method. Stanford University California 94305. Stanford. doi: 10.2514/1.34895
15. Tajima M, Ning Hu, Fukunaga H (2010) Experimental impact force identification of CFRP Stiffened Panels. J Jpn Soc Comp Mater doi:/10.6089//jscm.35.106
16. Ricordeau J, Lacaille J (2010) Application of random forests to engine health monitoring. Paper 730 ICAS. In: Proceedings of 27th international congress of the aeronautical sciences, 2010
17. Pankov AV, Svirskiy Yu A, Sorina TG (2015) The main results of researches on creation of onboard systems monitoring (SHM), including the use of fiber-optic sensors. Report on the international round table of the SKOLKOVO Institute of Science and Technology, effective methods for forecasting resource. Moscow. 14–15 May 2015 (in Russian)
18. Nyquist H (1928) Certain topics in telegraph transmission theory. Trans AIEE
19. Bryson AE, Denham WF, Dreyfus SE (1963) Optimal programming problems with inequality constraints. Necessary conditions for extremal solutions. AIAA, 2544–2550
20. Marquardt D (1963) An algorithm for least-squares estimation of nonlinear parameters. SIAM J App Math 11:431–441
21. Smola AJ, Scholkopf BA (2004) Tutorial on support vector regression. J Stat Comput 14 (3):199–222
22. Schmidt HJ, Schmidt-Brandecker B (2009) Design benefits in aeronautics resulting from SHM. In: Boller C, Chang F-K, Fujino Y (eds) Encyclopedia of structural health monitoring. Wiley, Chichester. ISBN: 978-0-470-05822-0, 1807-1813
23. Boller GA et al (2009) Commercial fixed-wing aircraft. In: Boller C, Chang F-K, Fujino Y (eds) Encyclopedia of structural health monitoring. Wiley. ISBN: 978-0-470-05822-0, 1917-1932
24. Sundaram R, Kamath GM, Gupta N, Subba RM (2010) Damage studies in composite structures for structural health monitoring using strain sensors. Advanced Composites Division, National Aerospace Laboratory, Bangalore
25. Takeda N (2008) Recent development of structural health monitoring technologies for aircraft composite structures. In: ICAS Proceedings of 26th international congress of the aeronautical sciences, Paper 706 (2008)
26. Nesterenko BG (2011) The requirements for the fatigue and durability of structures for civil aircraft. Scientific Bulletin of MSTU. Moscow, pp 49–59 (2011) (in Russian)
27. Nesterenko BG (2007) Fatigue and durability of longitudinal joints obshivka pressurized fuselages. In: Scientific Bulletin of MSTU. Moscow. pp 70–81 (2007) (in Russian)
28. Rajher VL, Selikhov AF, Khlebnikov IG (1984) Records of a plurality of structures critical indicators in the evaluation of durability and resource. In: Scientific notes of TSAGI XV. Publishing Department of TSAGI, Zhukovsky (in Russian)